



Exploration of the material transfer effect in local loading forming of ultra-large-size integrated component with multi-rib

Ke Wei¹ · Qing Ma¹ · Gaochao Wang¹ · Xiaoguang Fan²

Received: 3 January 2020 / Accepted: 19 May 2020 / Published online: 27 May 2020
© Springer-Verlag London Ltd., part of Springer Nature 2020

Abstract

Isothermal local loading forming is a less-loading and flexible forging technology, which is promising to form the ultra-large-size integrated component with multi-rib by adopting small tonnage equipment. Due to the local loading characteristic, the material in the loading region can transfer into the unloading region in the transitional region. Identifying the affect region of the material transfer is important to control the material flow and obtain high-quality components under local loading way. In this work, the phenomena of the material transfer are explored and the boundaries of the transitional region are clarified. Firstly, the material transfer after each loading step is analyzed by displacement field and strain field based on finite element simulation of the ultra-large component. Meanwhile, the velocity vectors during each loading step are observed. Secondly, the variations of the material volume in different loading zones during each loading step are revealed. Subsequently, the change of material volume located far from the die partition line is analyzed. Furthermore, the induced forming problems by the material transfer effect, i.e., folding and additional strain, are elaborated. Finally, the boundaries between the transitional region and first/second loading zone are determined. The phenomena of the material transfer and the induced folding in the transitional region are verified using an eigenstructure with multi-rib by the FE simulation and physical simulation experiment.

Keywords Ultra-large component · Multi-rib · Local loading forming · Material transfer effect · Transitional region

1 Introduction

To satisfy the ever-increasing demands of high performance and lightweight in aerospace industry, the structural components with multi-rib of titanium alloy have been widely used as a key load bearing structure in aircraft [1, 2]. Instead of the traditional multi-piece welded components, the integrated components are becoming the desirable load bearing structures to improve the strength uniformity of the components [3]. Owing to the integration of structural design, the size of these integrated components becomes ultra-large, such as the bulkhead. The plastic processing forming with hot die forging

is one of the main manufacturing technologies to fabricate this kind of components, which can not only reduce the cost due to nearly constant volume of the workpiece but also serve to tailor the service properties of metals through microstructure evolution [4, 5]. However, two main forming problems are encountered in the forming process in terms of ultra-large-size components, complex structure and difficult-to-deform property of titanium alloy, which can be described as follows:

- (1) The ultra-large-size component with multi-rib is very complex. The irregular and overlapped component requires the heavy-duty press with high stiffness and high energy.
- (2) Titanium alloys are difficult to form because of their high deformation resistance, low ductility, and strong microstructural sensitivity to processing.

Therefore, both of the forming problems may bring about a great challenge to acquire the components with high precision, high performance, and low cost. It is meaningful to adopt the advanced accuracy forming processing technology to address this challenge. To this end, the isothermal forming combined

✉ Ke Wei
weike@nchu.edu.cn

✉ Xiaoguang Fan
fxg3200@nwpu.edu.cn

¹ School of Aeronautical Manufacturing Engineering, Nanchang Hangkong University, Nanchang 330063, China

² School of Materials Science and Engineering, Northwestern Polytechnical University, Xi'an 710072, China

with local loading has been proposed by Yang et al. [6–8] to form this kind of components. In the processing of the isothermal forming by local loading, the top die or bottom die is separated into several parts; the loading force is only applied to the local zone of the billet, then the integrated component can be formed by switching the loading zones step by step, as shown in Fig. 1 [2]. Meanwhile, the workpiece is formed at a relatively low speed without die chilling due to the constant temperature. Therefore, the isothermal local loading forming (ILLF) technique provides a feasible way to form ultra-large-size integrated component with multi-rib using a hydraulic press with a small tonnage.

A typical ultra-large-size integrated component is shown in Fig. 2a. The length of the component is greater than 1300 mm, but the largest rib width is only 18 mm and the thickness of the webs is within the scope of 16–28 mm. In the process of the ILLF, there exist loading zone A and loading zone B. Due to the die structure of the local loading (as the clearance shown in Fig. 2b), the material can transfer from loading zone A into loading zone B when loading zone A is the deformation zone. Gao et al. [9, 10] pointed out that the transferred material can generate intense deformation inhomogeneity near the die partition line, which does not appear in the integral loading process. Besides, Gao et al. [11] also revealed that the folding defect can be produced easily because of the transferred material. Therefore, the material transfer plays a significant role in forming quality of the component under local loading way. Nevertheless, the development of this advanced forming process is restricted by the above flow-induced forming problems. To this end, exploration of the material transfer effect and determination of the boundaries between the transitional zone and first/second loading zone are favorable to further control the transferred material and realize the process optimization.

To date, much work has been carried out on the analysis of the inhomogeneous deformation and forming defect during

the local loading process. Sun et al. [12] explored the influences of the forging mode, friction value, and local loading pass on the final inhomogeneous deformation degree of the integral component after local loading forming. Sun and Yang [13] studied the filling of the rib by metal flow; the results showed that the integral component can be divided into the easy forming region and the difficult forming region. Using unequal-thickness billet for different forming regions can improve the capability of the die under-filling. Fan et al. [14] investigated the effect of deformation inhomogeneity on the microstructure and mechanical properties under local loading forming. Furthermore, Fan et al. [2] established a through-process macro-/micro-FE modeling to predict the macroscopic deformation and microstructure evolution in multi-step local loading forming process, which makes a great contribution to the development of the mechanisms of microstructure evolution for ILLF technology. However, the above researches pay little attention to the material plastic flow, especially near the die partition line.

As to the material flow nearby the die partition line, Zhang and Yang [15] revealed that the distribution of the material transfer from the loading zone into an unloaded zone is mainly determined by the geometric structure of the unloaded zone. However, the scope of the shifted material and subsequent induced forming problems are not analyzed. Gao et al. [11] revealed that the material flow from the loading zone into the unloading zone with opposite directions occurs in the one pass with twice loading steps sequentially. Gao et al. [16] also discussed that the reciprocating transverse flow of material can lead to forming defects, such as the folding. To eliminate the folding, Gao et al. [17] proposed an adaptive folding index to predict the folding quickly, and the avoidance measures are put forward by decreasing spacer block thickness and increasing friction. Wei et al. [18–20] revealed that the optimization of the billet volume is an effective way to avoid the folding and improve the deformation homogeneity near the die

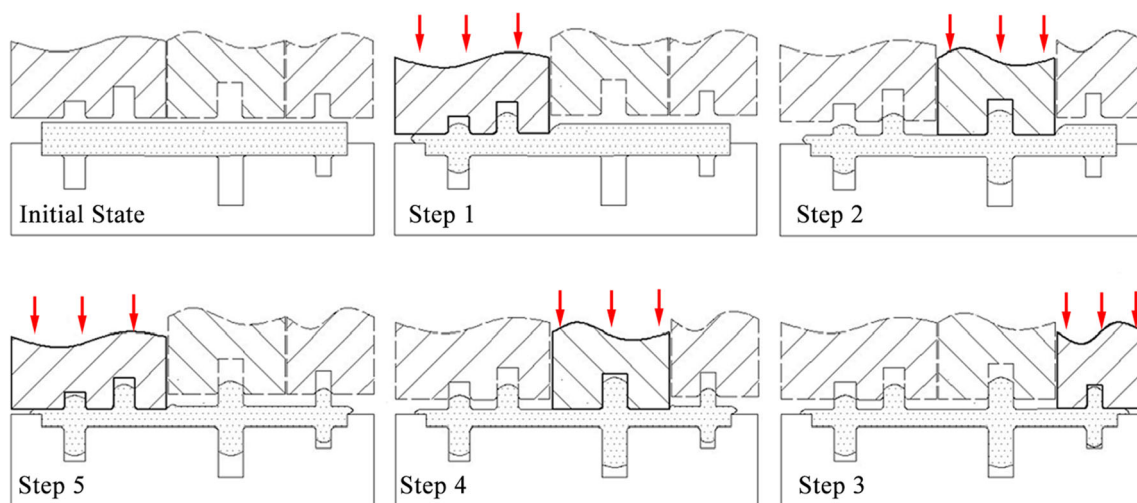
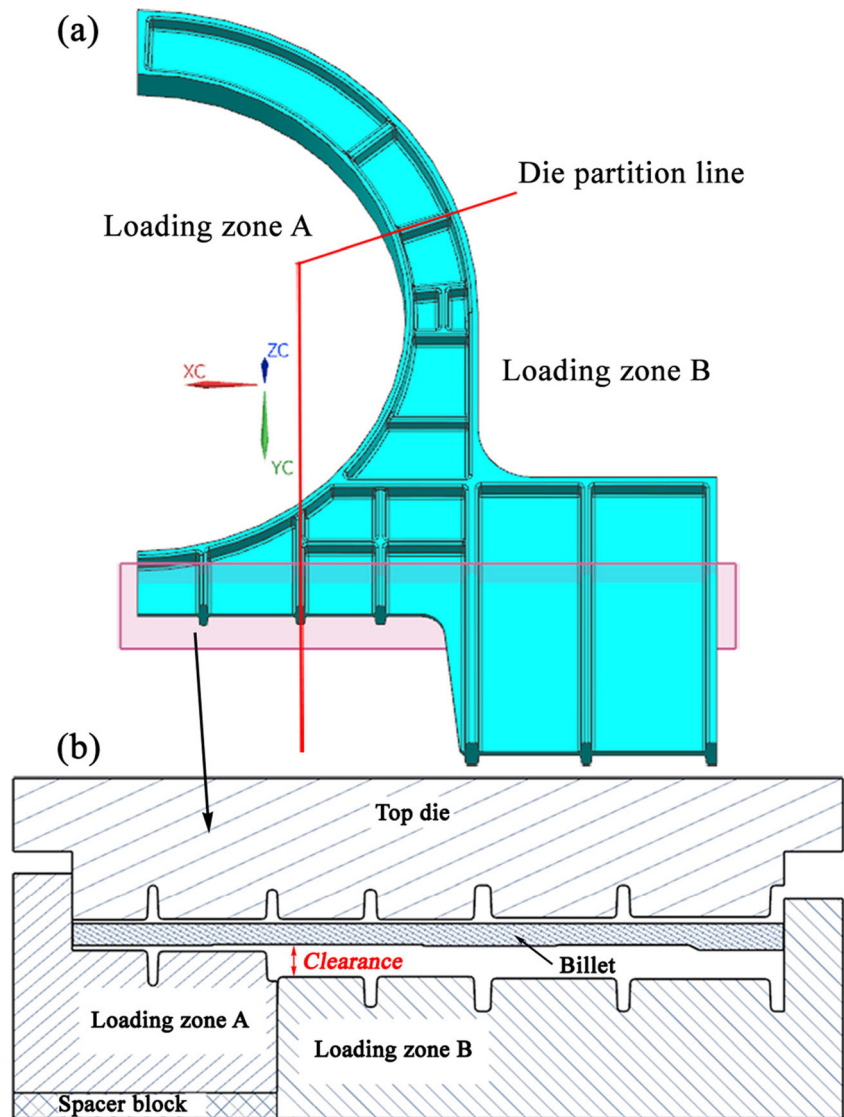


Fig. 1 Schematic diagram of the local loading process [2]

Fig. 2 Ultra-large-size integrated component with multi-rib (a) and schematic diagram of local loading forming (b) employed in this study



partition line. The above studies focus on the material flow behavior and defect generation that are close to the die partition line, providing the method references for the investigation of the material transfer. However, the used component in these works is relatively simple. For the ultra-large-size integrated component with multi-rib, the structural shape is extremely complicated; the change of the material volume by the material transfer in different loading zones should be considered and investigated, which are either close to the die partition line or far from the die partition line. Moreover, there is still a lack of extensive research on the material flow in terms of the ultra-large-size integral component during the local loading process. Meanwhile, the boundaries between the transitional region and first/second loading zone are not cleared. Hence, the material transfer process and the subsequent material volume change during the local loading process need further investigation.

The purpose of the present paper is to explore the material transfer effect during the local loading process for manufacturing the ultra-large-size integrated component with multi-rib. Based on the 3D finite element (FE) model, the material transfer during each loading step was investigated by using the velocity vectors combined with the displacement field (X -direction) and strain field. The variations of the material volume caused by material transfer in different loading zones were quantified. The folding and additional strain were analyzed and the boundaries between the transitional region and first/second loading zone were identified. This knowledge provides guidelines for ascertaining the characteristic of the material flow between different deformation zones, the mechanism of the induced forming problems, and the improvement of the forming quality during the local loading process.

2 FE modeling and local loading path

2.1 FE modeling

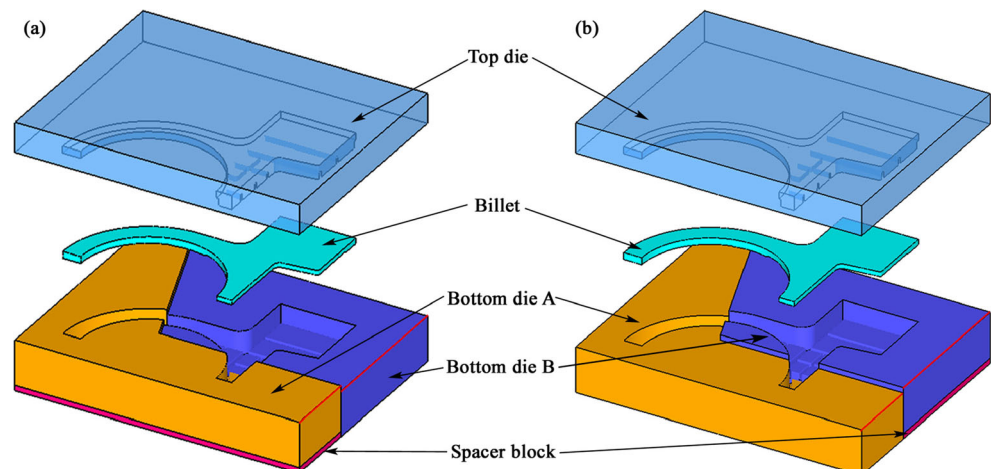
Nowadays, FE simulation is a powerful tool for predicting and analyzing the forming characteristics in material processing. The material flow variation and defect evolution can be observed based on the velocity vectors during the forming process. Based on FE simulation, the material flow behavior and folding defect formation during the integral die forging of asymmetrical flanges were investigated by Chan et al. [21]. In the multi-way loading forming of multi-cavity parts, Sun et al. [22] analyzed the velocity diagram under four representative loading paths, then the inhomogeneous deformation law of the material and forming defect generation mechanism was revealed accordingly. By FE simulation, Gao et al. [23] investigated the formation mechanisms of three typical types of folding defects (local-loading-type folding, confluence-type folding, and bending-type folding) based on the evolution of the velocity field. On this basis, the material transfer process under local loading forming is analyzed by the FE simulation method in this work.

In order to carry out the local loading on the single-action hydraulic press, the integral bottom die is divided into two parts and the spacer block is acted as the adjustor to locate under one of the parts, while the top die remains integral structure, as the assembled die shown in Fig. 3. Then, three steps are included during the local loading process, which are (1) the first loading step, (2) the spacer block removed step, and (3) the second loading step. In the first loading step, the spacer block is placed under the deformation zone, allowing one part of the bottom die to be protuberated. Before the second loading step, the spacer block is removed, which makes the two parts of bottom dies coplanar and the workpiece can be deformed only by the other part of the bottom die. Under the circumstances, the material processing method of the less-loading forming technology for the ultra-large component can be conveniently applicable in a single-action

hydraulic press. The spacer block is the key object and the critical step to achieving the local loading condition.

Because the filling of the cavity-rib is a typical bulk forming process, in which the plastic deformation is much larger than the elastic deformation, the current FE model is established based on the rigid viscoplastic variation principle. According to the guideline of literature [24], the billet is designed as an unequal-thickness billet to improve the die under-filling, which regarded as the rigid plastic deformation body. All the dies as well as the spacer block are regarded as the rigid body, then the elastic deformation can be ignored in FE simulation. During the local loading process, the Von Mises yield criterion and the isotropic hardening law are employed. The shear friction model is adopted to describe the friction behavior between the die and workpiece and the constant friction factor is defined as 0.5 based on the research by Zhang et al. [25]. According to the research by Sun et al. [26], the flashless forging mode was adopted and the die partition line was located in the rib of the component. The combined isothermal forming is executed under constant high temperature (970 °C) and a low-speed top die (0.2 mm/s). The variation of the temperature is neglected. The material of the billet utilized in the FE model is TA15 titanium alloy. The stress-strain curves of TA15 were obtained by isothermal compression test, which came from the work of Shen [27], as the stress-strain relations shown in Fig. 4. The flow stress of the TA15 under the different strains, strain rates, and deformation temperatures was obtained based on the self-contained interpolation function in FE simulation software. In the established FE model, the temperatures of billet and die are constant at 970 °C during the forming process, so that each element of the workpiece is within these temperature ranges. The constitutive curve of the 970 °C can be acquired by automatic interpolation in FE simulation. Additionally, the billet was discretized by tetrahedral elements, and the initial average mesh size was 1/4 to 1/5 of the widths of ribs. Meanwhile, an automatic remeshing technique is adopted to ensure computational efficiency and high mesh quality.

Fig. 3 FE model of the ultra-large-size integrated component with multi-rib under local loading: **a** path A; **b** path B



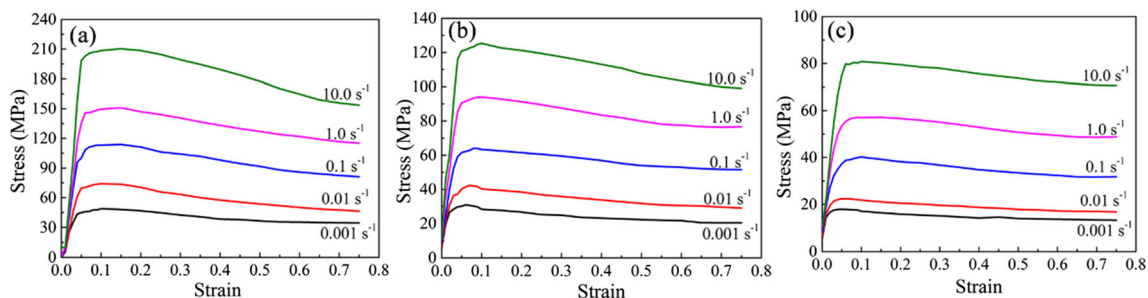


Fig. 4 Stress-strain curves of TA15 under different temperatures [27]: **a** 900 °C; **b** 950 °C; **c** 1000 °C

2.2 Local loading path

In order to quantitatively analyze the material transfer and reflect the volume change in the loading and unloading zones, two forming paths for the local loading are designed. Path A represents that the spacer block is placed below bottom die A during the first loading step, allowing bottom die A to be protuberated. Then the first deformation zone of the billet is above bottom die A, as shown in Fig. 3a. On the other hand, path B represents that the spacer block is placed below bottom die B during the first loading step, so the first deformation zone of the billet is above bottom die B instead, as shown in Fig. 3b. It can be recognized that path A and path B are different orders of local loading steps under the same deformation zones.

The major reason for the designed two loading paths is to research the effect of the material transfer on volume variation under different local loading orders. By using two designed loading paths in this work, the volume variations of the same deformation zone will be quantitatively compared and analyzed under different local loading orders. Additionally, the effect of transferred material on the distant area of the formed zone during the second loading step can be attainable by loading path B.

3 Material transfer phenomena under different loading paths

At the initial stage of the local loading, ten points are selected to study the variation range of the material flow and deformation degree, as illustrated in Fig. 5.

3.1 Material transfer in the first loading step (path a)

To study the material transfer from the deformation zone to the unloading zone in the first loading step, the velocity vectors combined displacement field and strain field are analyzed. As can be seen from Fig. 6a, the observed velocity vectors are in the stroke of 75%, which are contained in the loading zone. At the time, a neutral layer exists in the web and its location is close to the die partition line. The material in that web would

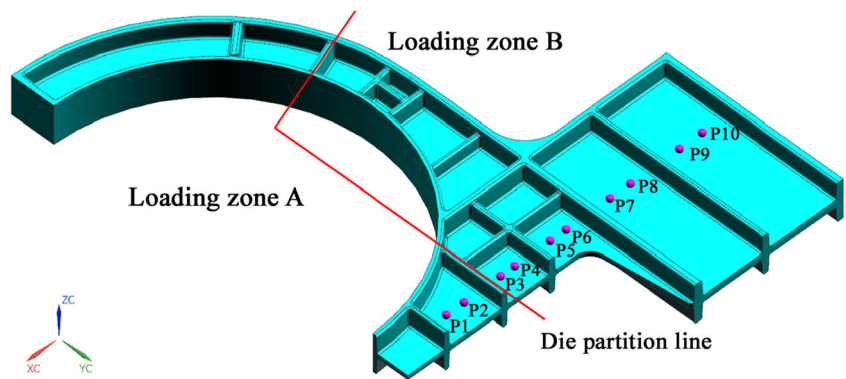
transverse flow along both sides of the neutral layer. The material in one side of the neutral layer can transverse flow into the adjacent rib of the die partition line in the loading region; however, that on the other side of the neutral layer can transverse flow into the unloading zone concurrently. Then, two flow patterns of the material can be observed after the material volume decreased in the loading zone. The one pattern is that the material flows and fills the cavity of the partitioned rib in the top die (flow I). The other pattern is that the material moves forward into the unloading zone (flow II). It can be seen in Fig. 2b that a clearance exists between the top die and one of the bottom die, then the transferred material in the unloading zone is not influenced by the die constraint and stays in free-flow state, which results in above-mentioned flow patterns continuous process until the end of the first loading step, as shown in Fig. 6b.

Figure 7 exhibits displacement field (X -direction) and strain field as well as their maximum values after the first loading step. Combined with field variables and maximum values, the gradient decreasing trends of the displacement and strain are shown in the unloading zone, i.e., the closer to the die partition line, the more significant of the displacement and strain in the unloading zone. Moreover, it can be seen from Fig. 7b that point 1 is in the opposite of all other points; this shifted point in the X -direction is caused by the material flow from the left side of the neutral layer in Fig. 6. Correspondingly, all points but point 1 are shifted by the material flow from the right side of the neutral layer. Besides, among all the selected points, the maximum strain is nearly 1.0, but that strain is less than 0.1 after point 4, as shown in Fig. 7d. With respect to the zone which is far from the die partition line, the effect of the displacement and strain by the transferred material is little, leading to an affect region near the die partition line, as the material transfer region shown in Fig. 7a.

3.2 Material transfer in the second loading step (path B)

Figure 8 shows the material flow during the second loading process. As can be seen from Fig. 8a, the observed velocity vectors are in the stroke of 75%, which are also contained in the loading zone. At the time, a neutral layer exists in the web and its location is closed to the die partition line. The material

Fig. 5 Location of the selected points in the component



in that web would transverse flow along both sides of the neutral layer. Similar to the first loading step, the material in left side of the neutral layer can transverse flow into the adjacent rib of the die partition line in the current deformation zone. That on the other side of the neutral layer can transverse flow into the unloading zone in the meantime, but that unloading zone is already formed during the first loading process under path B. Then, three flow patterns of the material can be observed after the material transfer from the deformation zone into the unloading zone. Comparing the first loading step under path A, it can be found that flow I and flow II are the same flow pattern, but there emerges a new flow pattern (flow III) which is the material flows and fills the cavity of the partitioned rib between the junction of two bottom dies. The reason for the appearance of the flow III pattern can be explained by two reasons, as follows:

- (1) The removed spacer block can lead to two upper surfaces of the bottom die staying in the same horizontal line, resulting in the die cavity of the partitioned rib formed completely between the junction of two bottom dies.

- (2) The transferred material of the first loading step is gathered nearby the die partition line. Thereby, the initial material volume of the second loading zone is increased, allowing more material to be filled into the die cavity of the partitioned rib.

Nevertheless, it is hard to form that cavity-rib during the first loading step because the corresponding cavity-rib is not formed. With the top die descending, it is interesting to observe that a new neutral layer and flow pattern produces close to the die partition line, as flow IV shown in Fig. 8b. This is because the clearance between the top die and bottom die in the unloading zone is gone, then, the loading mode is similar to the integral loading process between the partitioned rib with its adjacent rib.

Figure 9 exhibits displacement field (X -direction) and strain field as well as their maximum values after the second loading step. It is notable that remeshing is conducted before the top die descending in FE simulation so as to catch the strain accumulation during the single second loading step merely, which means that the strain generated in the first

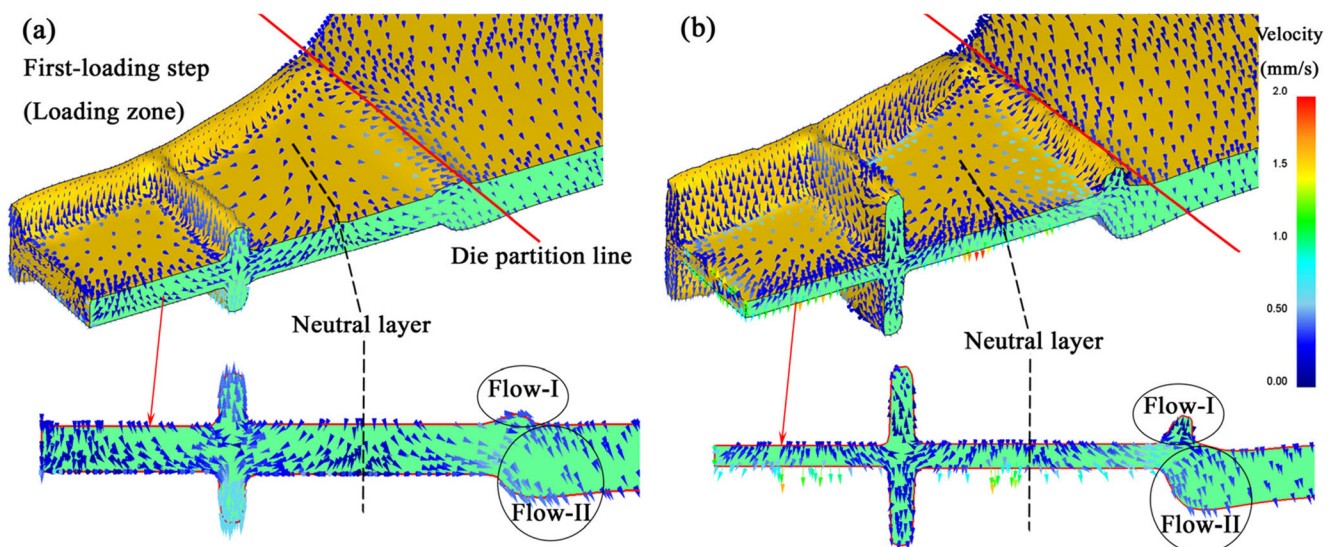


Fig. 6 The velocity vector of the first loading step under path A: **a** stroke of 75%; **b** stroke of 100%

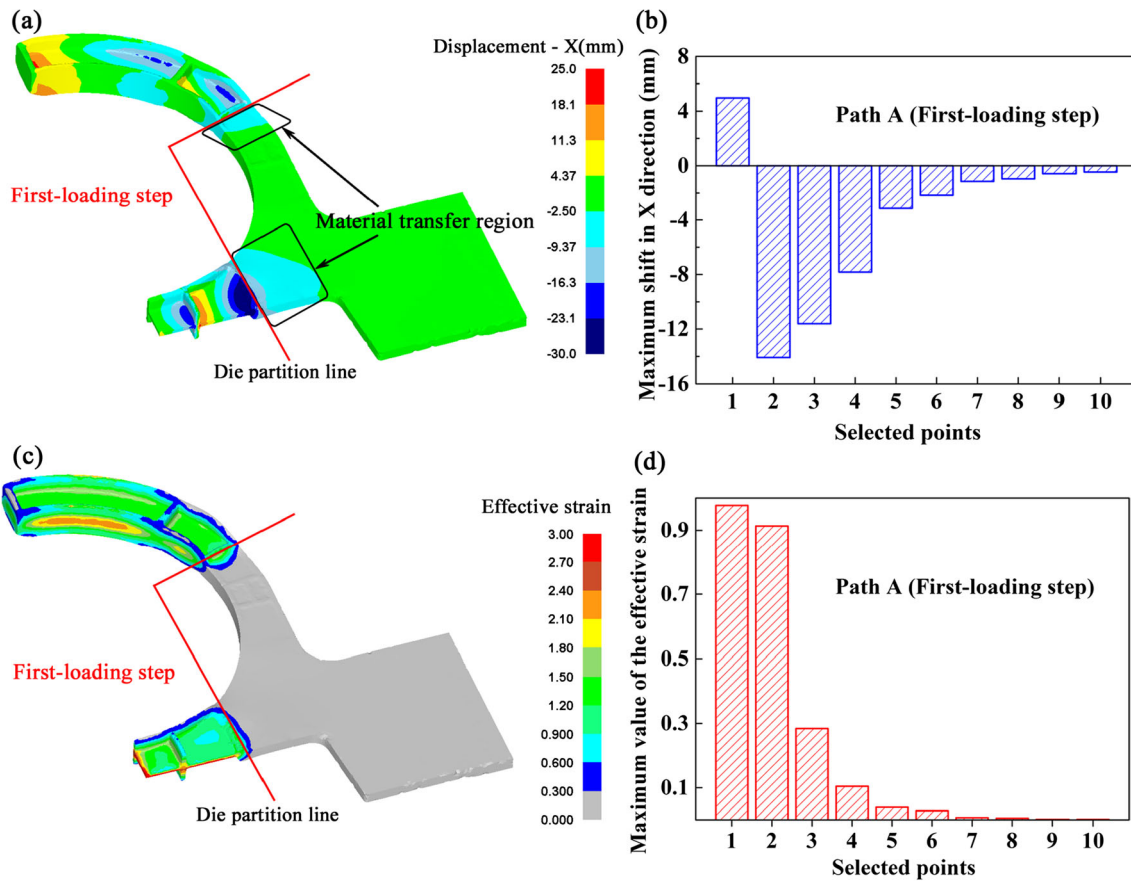


Fig. 7 Forming results after the first loading step under path A: **a** X-direction displacement variation; **b** maximum shift in X-direction; **c** strain variation; **d** maximum value of the effective strain

loading step is cleared. Combined with field variables and maximum values, the gradient decreasing trends of the displacement (Fig. 9a) and strain (Fig. 9c) are also observed in the unloading zone, but limited from the die partition line to

the first rib of the unloading zone. From the observation of the maximum values in Fig. 9b, like the first loading step, point 1 is in the opposite of all other points by the displacement variation. This shifted point in X-direction is caused by the

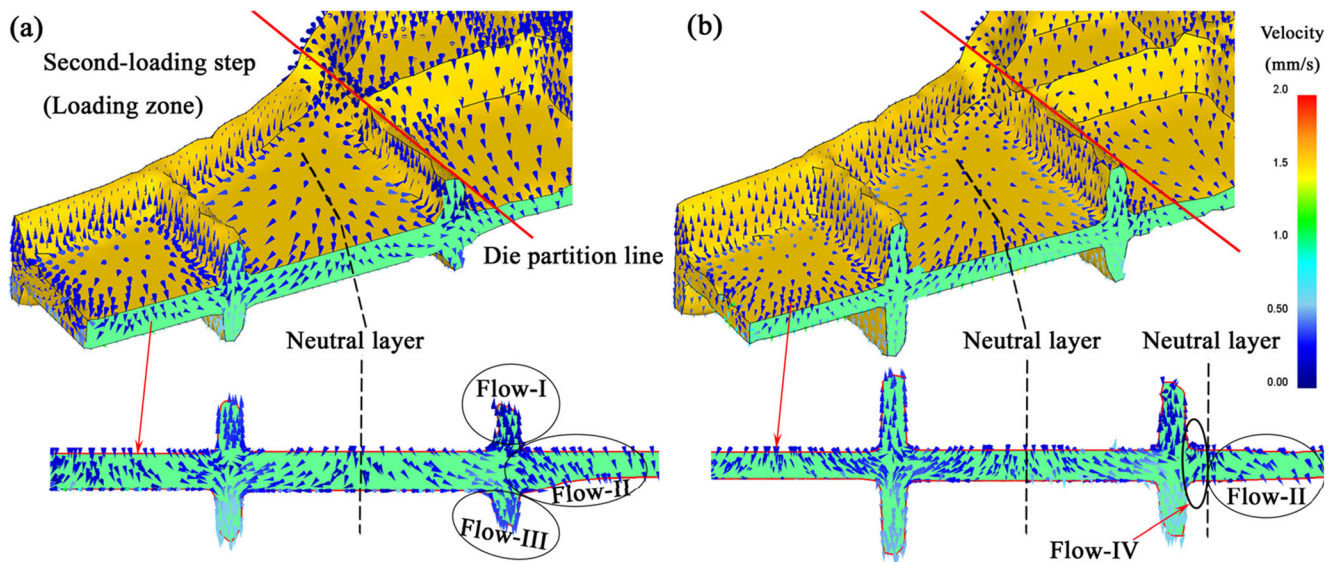


Fig. 8 The velocity vector of the second loading step under path B: **a** stroke of 75%; **b** stroke of 90%

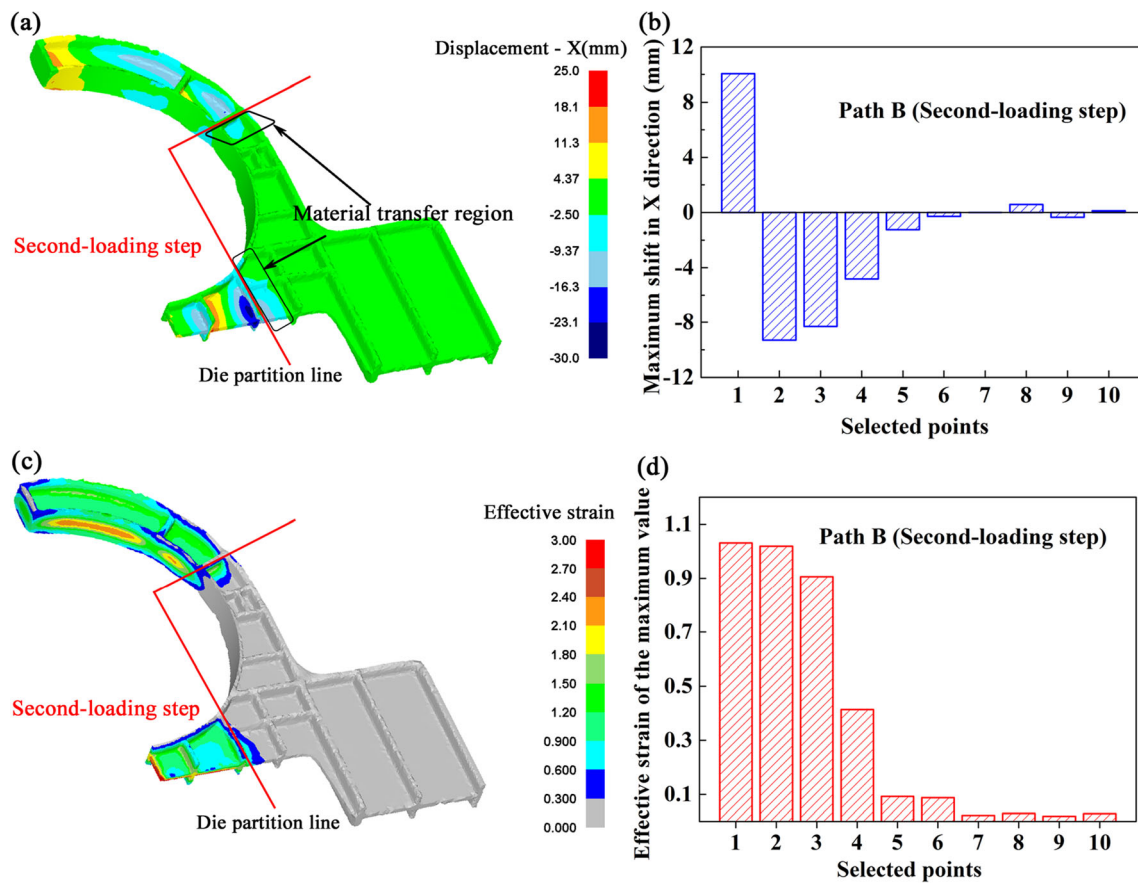


Fig. 9 The forming results after the second loading step under path B: **a** X-direction displacement variation; **b** maximum shift in X-direction; **c** strain variation; **d** maximum value of the effective strain

material flow from the left side of the neutral layer in Fig. 8a. Correspondingly, all points but point 1 are shifted by the material flow from the right side of the neutral layer and move forward into the unloading zone. The points from 1 to 4 are significant, but the points from 5 to 10 are very close to zero. The reason for this phenomenon is that the adjacent ribs (double-side ribs) of the die partition line are already shaped during the first loading step, then, material flow II pattern is inevitable to confront with the resistance of the shaped ribs. The material in the unloading zone is thus barely shifted beyond the shaped ribs and the strain in that zone is barely accumulated. Consequently, no resistance of the shaped rib exists during the first loading step and the affect region by the material transfer during the first loading step is larger than the second loading step.

In this work, because the clearance exists between the top die and one part of the bottom die, the material transfer is inevitable during the local loading process. This is the fundamental reason for the second pattern generated. In the research of Gao et al. [16] and Wei et al. [19], their results showed that the severity of the folding is mainly dependent on the quantity of the transferred material. Moreover, the back-flow material of the fourth pattern is derived from the transferred material.

Therefore, it can be concluded that the patterns of material flow II and flow IV are related to the forming defect under local loading way. As for the integral loading way, it can be seen from Fig. 10 that first and third patterns of the material flow are filled the cavity of the partitioned rib in the top and bottom die, respectively. The patterns of material flow I and flow III under integral loading are the same as those material flow under local loading. Therefore, flow I and flow III by the local loading have the same effect with the integral loading.

3.3 Material volume change in unloading zones

The above analysis about the material transfer phenomena reveals that reciprocal transfer process can be observed between two loading steps, which suggests that there exists an interaction between the loading zone and unloading zone. The material transfer effect by the alternative loading die can lead to volume distribution variation between different loading zones. Consequently, the inhomogeneous deformation can be aggravated and induced defect can be generated near the die partition line. Therefore, it is necessary to understand the detailed variation process of the volume distribution in the unloading zone.

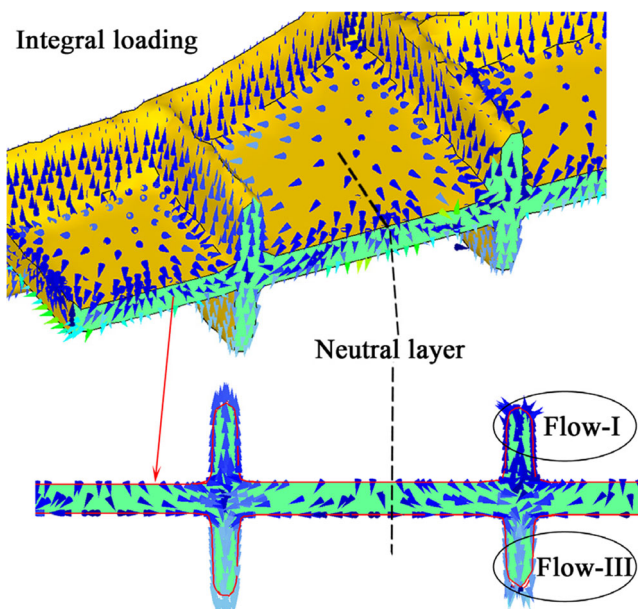


Fig. 10 The velocity vector during the integral loading process

Figure 11a illustrates the increasing rate of the material volume in unloading zones during local loading forming. Notably, the calculated volume during the first loading step is under path A, while the calculated volume during the

second loading step is under path B. It can be seen that the material volume in the unloading zone increases gradually with the increase of top die before the end of the stroke. Between two loading paths, that material volume under path B is increased faster. The reason can be explained from the comparison of the initial volume under two loading paths, which are illustrated in Fig. 11b–d. Due to the material transfer during the first loading step under path B, the initial material volume under path B (V^{2nd_BL}) in the unloading zone is larger than path A (V^{1st_AL}), especially near the die partition line.

Additionally, at the end of the top die stroke, the material volume in unloading zone is continuously increased under path A; however, it decreased under path B. The above phenomenon can be accounted for the reasons below:

- (1) During the material transfer process under the first loading step of path A, there is no die constraint under the projection of the unloading zone. The free-flowing state of the transferred material is continuous to the end of the first loading step, allowing the material volume to be increased during the whole course of the first loading step in the unloading zone.
- (2) At the later period of the second loading step under path B, the transferred material would contact with top die and

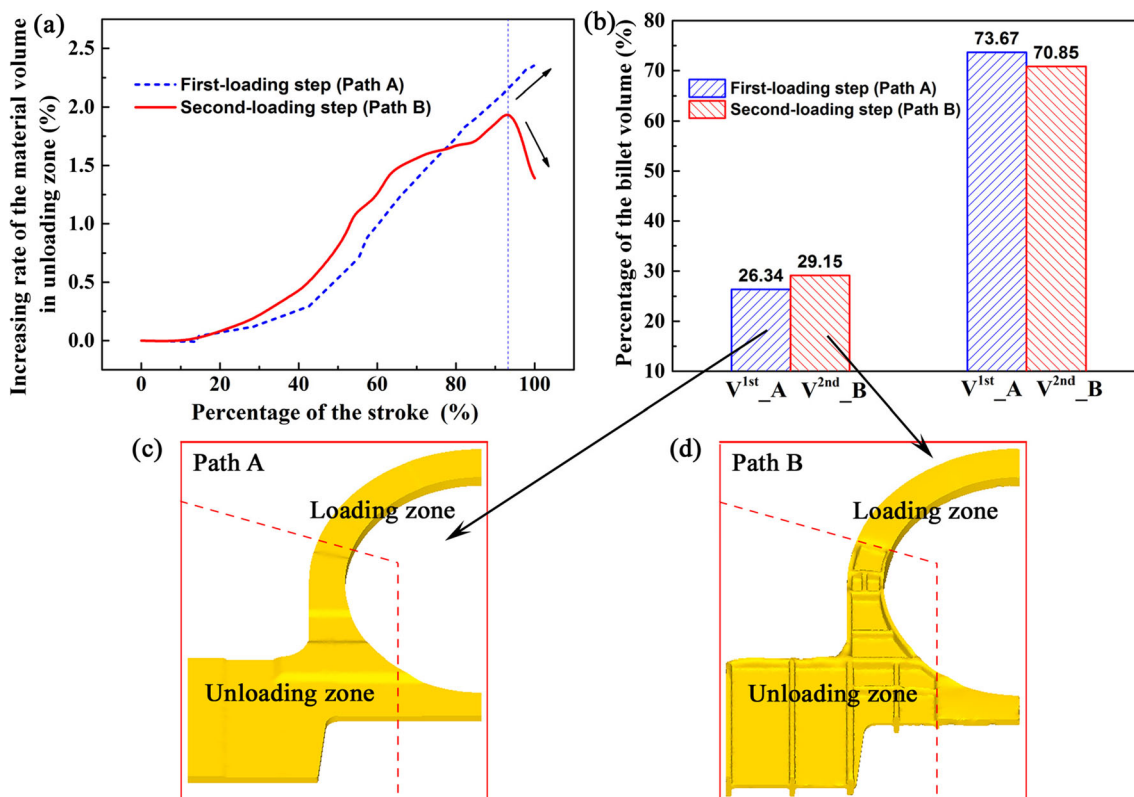


Fig. 11 Material volume variation in unloading zones: a increasing rate of material volume in unloading zones; b volume ratio of different zones before local loading; c billet shape at the beginning of first loading step under path A; d workpiece at the beginning of second loading step under path B

bottom die simultaneously. Subsequently, a new neutral layer is generated and one part of the material back-flow into the loading zone, as shown in Fig. 8b. Under this circumstance, the material volume of the unloading zone is decreased since the neutral layer generated until the end of the die stroke.

3.4 Material volume variation far from the die partition line

In order to investigate the effect of transferred material on the distant area (away from the location of the die partition line) in unloading zone, the objective zone from the middle of p7 and p8 to the edge of the workpiece is selected for calculating the volume variation and observation of the material flow, as the observed part shown in Fig. 12a. By comparing with the integral loading, it can be seen from Fig. 12b that the volume variation of the observed part appears in little differences by two local loading paths. When the stroke of top die reaches 65%, the volume in the objective zone is increased under the different loading steps as well as the different load patterns. The reason for the increased volume is because those materials are out of the objective zone flow into the objective zone, as the velocity field shown in Fig. 13a. With the top die descending, the volume in the objective zone is reversed to decrease until the end of the loading. This can be explained by observing the velocity vectors during the forming process, as the stroke of 95% shown in Fig. 13b. The longitudinal rib located between the P8 and P9 is fully filled at that time, then, the material is compelled to reverse the flowing direction due to the flow resistance of formed longitudinal rib. Under the circumstances, the material in the observed part flows out of the observed part; thus, the volume is gradually decreased and finally less than the initial volume of the billet.

Comparing the material volume variation of the observed part under different loading patterns and loading steps, a

conclusion can be drawn that no more additional material transfers from the loading zone into the distant area of the unloading zone during both local loading steps. Furthermore, switching the loading sequence of the first and second steps is not significant on the material flow in the unloading zone which is away from the die partition line.

4 Folding and additional strain by the material transfer effect

4.1 Folding

During the material transfer process of the first loading step, there is non-folding observed under both loading paths. Thereby, the folding may only occur during the second step. Figure 14 exhibits the generated folding by the material transfer effect under path A in the stroke of 90%. The black gray on the web means that the workpiece contacts with the two bottom dies at the moment. Because the clearance exists between the top die and one part of the bottom die, the type of material flow II (as shown in Fig. 8a) is inevitable during the local loading process. Subsequently, a confluence zone is formed between the contact surface and noncontact surface with the bottom die, resulting in the folding in the web near the die partition line. The detailed formation mechanism of the folding under the local loading way is described by Gao et al. [16] and Wei et al. [19]. Their results showed that the severity of the folding is mainly dependent on the quantity of the transferred material. Therefore, it can be concluded that the pattern of material flow II is related to the folding defect under the local loading way.

Avoiding the folding defect is desired for application of the isothermal local loading forming technology. If the transferred material is less than a specific value, the folding might be avoided. Four approaches were put forward to adjust and control the transferred material and eliminate the folding defect in

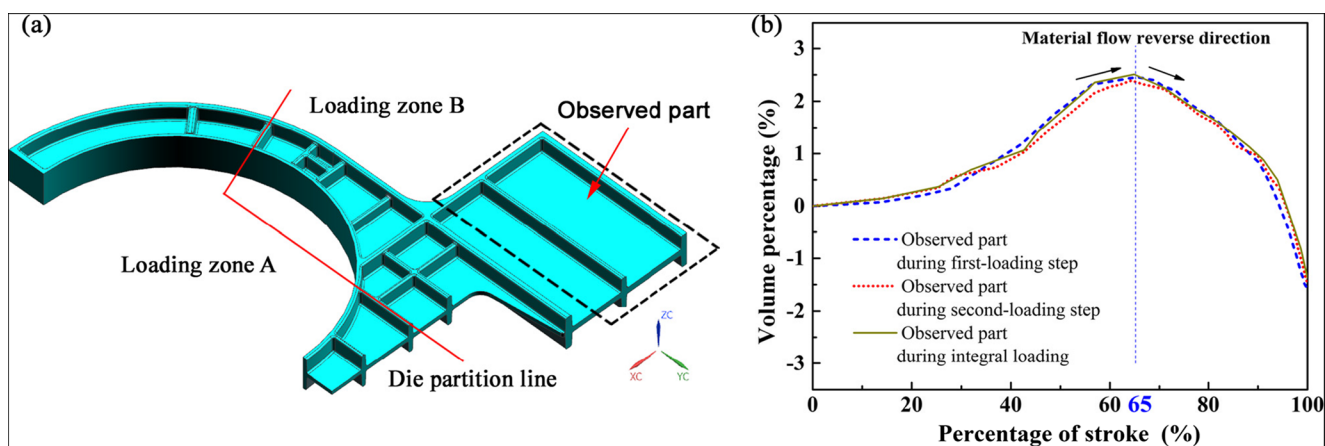
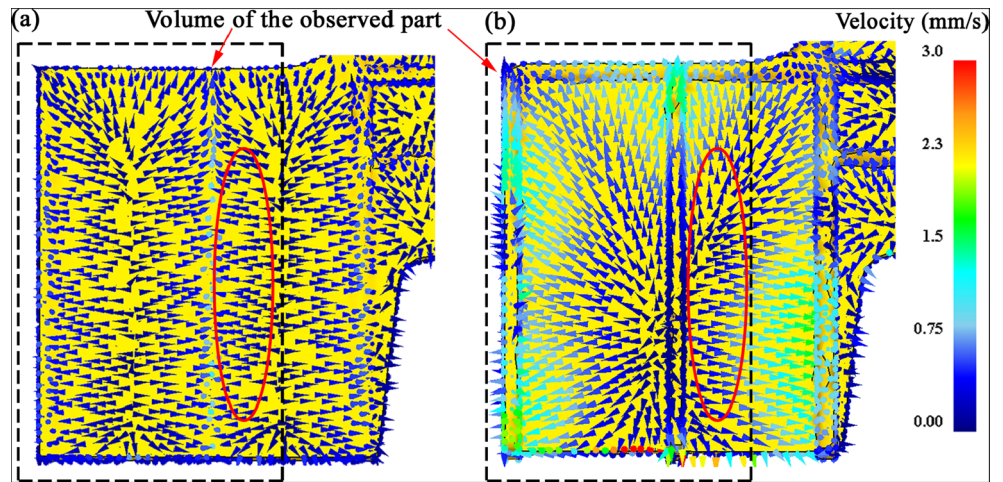


Fig. 12 Change rate of the observed part with the changing of the stroke during the first (path A), second (path B), and integral loading processes: **a** description of the observed part; **b** volume percentage of the observed part

Fig. 13 Velocity vector of the observed part far from the die partition line: **a** stroke of 65%; **b** stroke of 95%



the transitional region: (1) optimization of the initial billet volume; (2) increasing loading pass to obtain smaller reduction amount; (3) increasing friction factor; (4) increasing the fillet radius of the bottom die. The detailed process of solving the folding defect can be found in the references [16, 19].

4.2 Additional strain

As in the above analysis of the material transfer effect, the transferred material during the first loading step would be gathered near the die partition line in the unloading zone, resulting in the initial volume in that zone to be redistributed. Moreover, the transferred material during the second loading step can be produced by passive deformation, which means that the additional strain would be generated in the unloading zone owing to the material transfer effect. Under the circumstance, the intense inhomogeneous deformation can be induced by the reciprocal transferred material, then the strain

field and corresponding formation of the microstructure are thus discrepant with those zones that has no effect by the material transfer. So, comparing the strain field distribution of local loading and integral loading is beneficial to acquiring the difference of the accumulated strain in different deformation zones.

The comparison of the strain field in the traverse section by local loading and integral loading is presented in Fig. 15. Notably, the strain fields of the local loading under path A in Fig. 15b and path B in Fig. 15c are accumulated by both loading steps. Compared with the integral loading in Fig. 15a, the results show that the different ranges of local loading under path A are from the partitioned rib to its connected web in unloading zone, while the different ranges of local loading under path B are from the partitioned rib to the connected web which is between the first rib and second rib in the unloading zone. Besides, the strain field distribution in other zones by both paths of the local loading is almost the same as the integral loading.

Fig. 14 Folding generation in unloading zone during the second loading step (path A)

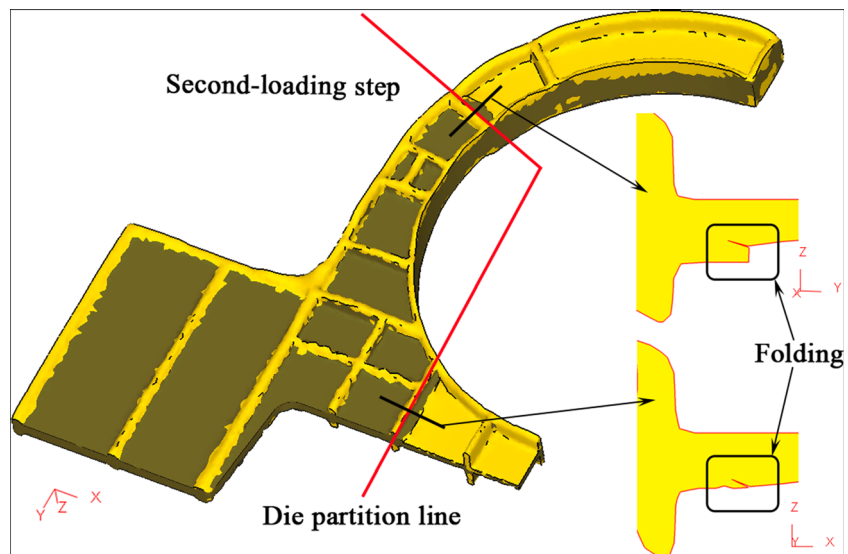
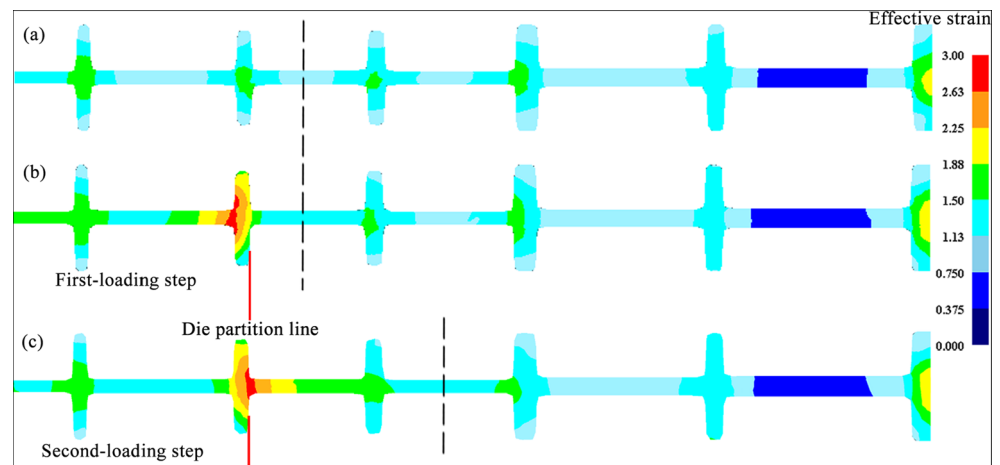


Fig. 15 Comparison of the strain field in the traverse section: **a** integral loading; **b** local loading under path A; **c** local loading under path B



Additionally, the accumulated strain near the die partition line is larger than the other zones with the same reduction rate during the local loading process. Actually, this phenomenon is bad for forming the quality of the ultra-large components, because the larger effective strain can lead to non-uniform microstructure to the ultra-large-size integrated component under local loading way, and thus affecting the whole mechanical properties of the final components. In order to decrease the additional strain and thus improve the deformation homogeneity in local loading, the billet and die parameters near the die partition line were optimized in our previous works [9, 18]. And they were approved to be effective approaches for decreasing the additional strain near the die partition line after local loading.

5 Boundary of the transitional region

According to the above analysis, it can be stated that the material transfer effect plays a fundamental role in the forming quality of the ultra-large-size integrated component under local loading way. The material flow history and strain state have large differences by different loading patterns near the die partition line. To study the induced forming defects purposefully by the local loading characteristics, clarifying the affected region by the material transfer effect and identifying the boundaries of the transitional region are very important in the research of the local loading forming. The reason can be explained as follows:

- (1) Due to the special forming problems existing near the die partition line, the design of the billet volume distribution and die parameters can be carried out in combination with multi-objective optimization method in the transitional region.
- (2) Taking the transitional region of the ultra-large-size integrated component as a research object in FE simulation

would shorten the computation time and reduce the computation storage.

- (3) The proportion in the projected area of the transitional region is small, which can be divided into smaller element size during the meshing in FE simulation so as to catch the detailed information of the forming results.
- (4) Instead of the integral ultra-large component, the transitional region can be extracted as an independent analysis object in the experiment observation, which is beneficial for saving experiment cost and reducing experimental intensity.

To reflect the forming characteristics under the condition of local loading, the material transfer effect should have no influence out of the boundary of the transitional region. Thus, the affected region by the material transfer effect should exceed the integral loading pattern. In this work, four aspects are considered in the identification of the boundary of the transitional region.

Firstly, from the perspective of the displacement (X -direction) field and strain field, the gradient decreasing trend of the displacement and strain can be visible in the unloading zone near the die partition line in both loading steps, as shown in Figs. 6 and 8. So the material transfer has a positive effect on these areas. Secondly, the displacement (X -direction) field and strain field were unchanged in the distant area of the unloading zone during both local loading steps. Therefore, those areas away from the die partition line were only deformed in one single loading step; the material transfer has no effect on those areas. On the other side, switching the loading order of the first and second steps is not significant on the material flow and volume variety in the unloading zone which is away from the die partition line. So, those areas can be regarded as the integral loading state and have no relationship with the transitional region. Thirdly, during the second loading step, the transferred material could flow into the cavity of the formed rib of the first loading zone which is adjacent to the die partition line. Hence, the transitional region should contain the closest ribs of the die

partition line. Lastly, due to the resistance of the formed rib of the first loading zone which is adjacent to the die partition line, the transferred material is hardly flowing over the cavity of that rib.

Based on the above analyses, the location of the transitional region can be defined next to the adjacent rib of the die partition line, i.e., the second web of both sides of the die partition line, as the vertical dashed lines shown in Fig. 15c. Due care should be paid to that strain should be accumulated by both loading steps in the transitional region.

6 Validation of the material transfer under local loading

In order to validate the material transfer behavior and subsequent folding defect under local loading conditions in the transitional region, a typical eigenstructure with multi-rib was designed, as shown in Fig. 16a. The length and width of the eigenstructure are 240 mm and 50 mm, respectively. The dimension feature of the eigenstructure is complex because the depth/width ratios of the ribs, the thicknesses of some webs, and distances between each rib are not the same; meanwhile, the crisscross ribs consist in the eigenstructure. In FE modeling, the local loading conditions and simulation parameters of the eigenstructure are in accordance with ultra-large-size integrated component in Fig. 3, such as the die partitioning line along the rib, closed die mode, loading die

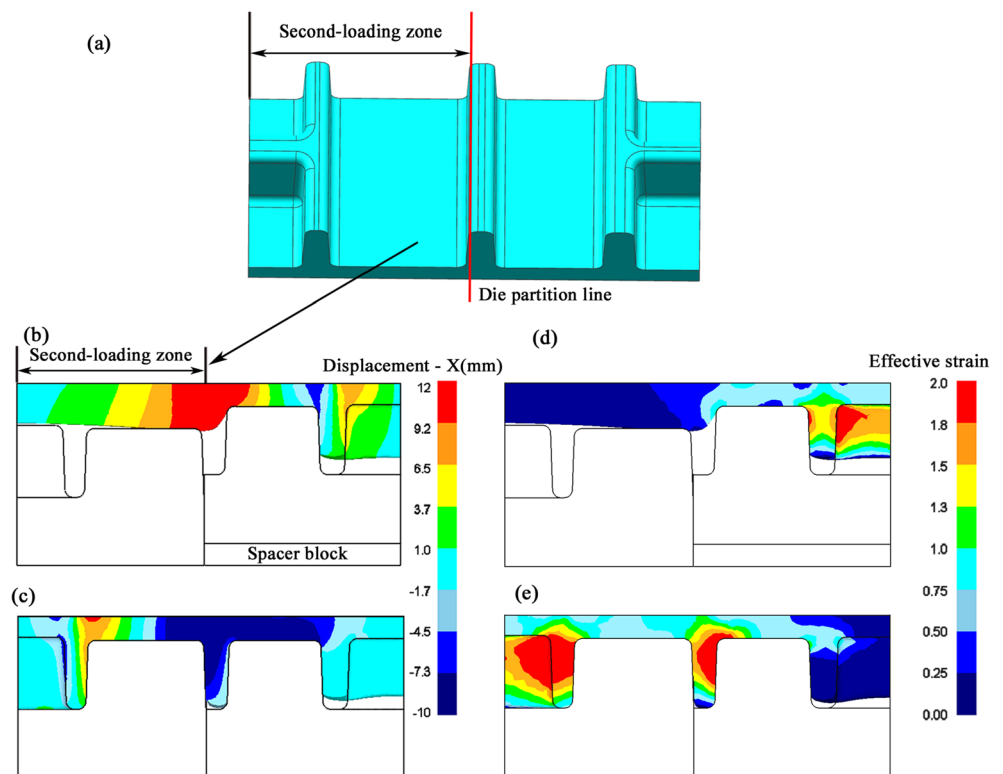
speed, and friction factor. The simple equal-thickness billet is adopted to observe the distribution of the displacement field and strain field.

After the first loading step, the gradient decreasing trends of the displacement (X -direction) and strain are visible in the unloading zone, as shown in Fig. 16b, d. Besides, it can also be seen that the affected region by the material transfer effect is contained in the unloading zone. During the second loading step, the strain generated in the first loading step is also cleared. Similar to the first loading step, the gradient decreasing trends of the displacement (X -direction) and strain are visible in the formed zone, as shown in Fig. 16c, e. The affected region by the material transfer effect is also contained in the formed zone. Therefore, the eigenstructure is within the transitional region of the local loading condition.

Moreover, the patterns of flow I, flow II, and flow IV are also observed during the second loading step in the analysis of the simulated result with the velocity vectors, as shown in Fig. 17a, b. It is not difficult to perceive that the folding is produced near the die partition line in the unloading zone during the second loading step. The locations of the folding in two components are both produced near the die partition line in the unloading zone during the second loading step.

Additionally, the physical simulation experiment was conducted to verify the folding by the transferred material during the second loading step. Dutta and Rao [28] pointed out that the flow behavior of lead at room temperature is similar to that of titanium alloy at elevated temperature. Sun et al. [12] and

Fig. 16 Forming results of the eigenstructure after first loading step and second loading step: **a** the eigenstructure; **b, c** X -displacement field; **d, e** strain field



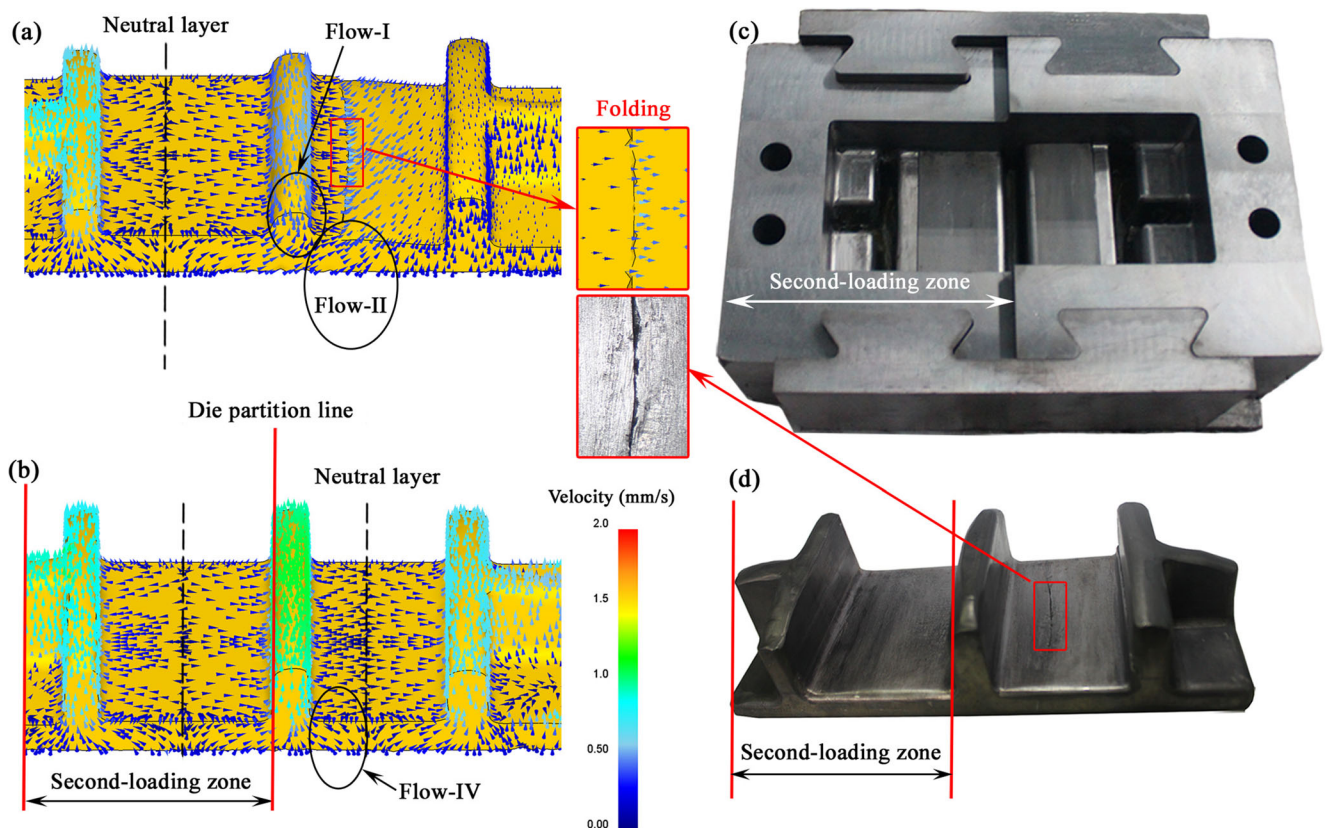


Fig. 17 The velocity vector and physical experiment of the eigenstructure: **a**, **b** the velocity vector under the stroke 60% and 90% of the second loading step, respectively; **c** assemble die for physical experiment; **d** experimental result

Zhang et al. [29] have successfully studied the forming characteristics of titanium alloy with T-shaped components under the local loading condition by using the lead as model material. Therefore, the lead in room temperature is selected to replace the titanium alloy at high temperature in this work. The material of die for experiment is 5CrNiMo, and the assemble die for physical experiment is depicted in Fig. 17c. The result of the local loading reveals that the folding is produced in the unloading zone, as shown in Fig. 17d.

Based on the above analysis, it can be concluded that the similar relation of eigenstructure component and ultra-large-size integrated component can be reflected in the process design, material flow behavior, displacement and strain fields, and folding evolution in the transitional region under local loading. So, the eigenstructure with multi-rib can effectively reflect and validate the phenomena of the material transfer and the induced folding in the transitional region under the local loading condition, which can also demonstrate that the material transfer effect is inevitable during the local loading process. Therefore, exploration of the material transfer effect in the local loading forming process is meaningful and provides guidelines for improving or eliminating the forming problems in the development of the isothermal local loading forming technology for ultra-large-size components with multi-rib.

7 Conclusion

In this paper, the material transfer from the loading zone into the unloading zone during the local loading forming was investigated and explored. Based on the results, the following conclusions can be inferred:

- (1) Four different patterns of the material flow can be produced during the local loading forming: (I) the material flows and fills the cavity of the partitioned rib in the top die; (II) the material moves forward into the unloading zone; (III) the material flows and fills the cavity of the partitioned rib in the bottom die; (IV) the transferred material back-flow into the loading zone at the later period of the second loading step.
- (2) Comparing the two local loading steps, the material volume of the unloading zone increases faster by the second loading step. The material volume of the unloading zone is continuously increased under the first loading step, but it decreased under the second loading step at the end of the top die stroke.
- (3) Due to the resistance of the shaped rib in the unloading zone during the second loading step, the gradient decreasing trends of the displacement and strain were

visible in the unloading zone near the die partition line in both loading steps. No additional material transfers from the loading zone into the distant area of the unloading zone during both local loading steps. Switching the loading sequence of the first and second steps is not significant on the material flow in the unloading zone which is away from the die partition line. Based on the above three points, the boundary location of the transitional region is defined at the second web of both sides of the die partition line.

Funding information This paper was financially supported by the Natural Science Foundation of Jiangxi Province (No. 20192BAB216023), Natural Science Foundation of China (No. 51975267, No. 51965043), and PhD Starting Foundation of Nanchang Hangkong University (No. 2030009401056).

References

- Shen GS, Furrer D (2000) Manufacturing of aerospace forgings. *J Mater Process Technol* 98:189–195
- Fan XG, Yang H, Gao PF (2014) Through-process macro-micro finite element modeling of local loading forming of large-scale complex titanium alloy component for microstructure prediction. *J Mater Process Technol* 214(2):253–266
- Yuan SJ, Fan XB (2019) Developments and perspectives on the precision forming processes for ultra-large size integrated components. *Int J Extrem Manuf* 022002(1):1–18
- Chen F, Cui Z, Chen J (2014) Prediction of microstructural evolution during hot forging. *Manufacturing Rev* 1(6):1–21
- Chen F, Ren FC, Chen J, Cui ZS, Ou HA (2016) Microstructural modeling and numerical simulation of multi-physical fields for martensitic stainless steel during hot forging process of turbine blade. *Int J Adv Manuf Technol* 82(1–4):85–98
- Yang H, Fan XG, Sun ZC, Guo LG, Zhan M (2011) Recent developments in plastic forming technology of titanium alloys. *Sci China Technol Sci* 54(2):490–501
- Yang H, Fan XG, Sun ZC, Guo LG, Zhan M (2011) Some advances in local loading precision forming of large scale integral complex components of titanium alloys. *Mater Res Innov* 15(S1):493–498
- Zhang DW, Fan XG (2018) Review on intermittent local loading forming of large-size complicated component: deformation characteristics. *Int J Adv Manuf Technol* 99(5–8):1427–1448
- Gao PF, Li XD, Yang H, Fan XG, Lei ZN (2016) Influence of die parameters on the deformation inhomogeneity of transitional region during local loading forming of Ti-alloy rib-web component. *Int J Adv Manuf Technol* 90(5–8):2109–2119
- Gao PF, Liu ZF, Lei ZN (2017) Deformation characteristics of transitional region during local loading forming of Ti-alloy rib-web component on the double-action press. *Int J Adv Manuf Technol* 93(1–4):559–569
- Gao PF, Yang H, Fan XG (2014) Quantitative analysis of the material flow in transitional region during isothermal local loading forming of Ti-alloy rib-web component. *Int J Adv Manuf Technol* 75(9):1339–1347
- Sun ZC, Yang H, Sun NG (2009) Simulation on local loading partition during titanium bulkhead isothermal forming process. *J Plast Eng* 16(1):138–143 (in Chinese)
- Sun ZC, Yang H (2009) Forming quality of titanium alloy large-scale integral components isothermal local loading. *Arab J Sci Eng* 34(Number 1C):35–45
- Fan XG, Yang H, Sun ZC, Zhang DW (2010) Effect of deformation inhomogeneity on the microstructure and mechanical properties of large-scale rib-web component of titanium alloy under local loading forming. *Mater Sci Eng A* 527(21–22):5391–5399
- Zhang DW, Yang H (2014) Distribution of metal flowing into unloaded area in the local loading process of titanium alloy rib-web component. *Rare Metal Mater Eng* 43(2):296–300
- Gao PF, Yang H, Fan XG, Lei PH (2014) Forming defects control in transitional region during isothermal local loading of Ti-alloy rib-web component. *Int J Adv Manuf Technol* 76(5):857–868
- Gao PF, Yang H, Fan XG (2015) Quick prediction of the folding defect in transitional region during isothermal local loading forming of titanium alloy large-scale rib-web component based on folding index. *J Mater Process Technol* 219:101–111
- Wei K, Fan XG, Zhan M, Yang H, Gao PF (2017) Improving the deformation homogeneity of the transitional region in local loading forming of Ti-alloy rib-web component by optimizing unequal-thickness billet. *Int J Adv Manuf Technol* 92(9–12):4017–4029
- Wei K, Zhan M, Fan XG, Yang H, Gao PF, Meng M (2018) Unequal-thickness billet optimization in transitional region during isothermal local loading forming of Ti-alloy rib-web component using response surface method. *Chin J Aeronaut* 31(4):845–859
- Wei K, Fan XG, Zhan M, Zeng X, Jiang XQ (2018) Uncertainty analysis and multi-objective billet robust optimization for transitional region of multi-rib component under isothermal local loading forming. *Int J Adv Manuf Technol* 97(1–4):1165–1179
- Chan WL, Fu MW, Lu J, Chan LC (2009) Simulation-enabled study of folding defect formation and avoidance in axisymmetrical flanged components. *J Mater Process Technol* 209(11):5077–5086
- Sun ZC, Cao J, Wu HL, Yin ZK (2018) Inhomogeneous deformation law in forming of multi-cavity parts under complex loading path. *J Mater Process Technol* 254(11):179–192
- Gao PF, Fan XG, Fei MY, Zhan M, Li YK (2019) Formation mechanisms and rules of typical types of folding defects during die forging. *Int J Adv Manuf Technol* 104(5):1603–1612
- Wei K, Yang H, Fan XG, Gao PF (2015) Unequal thickness billet design for large-scale titanium alloy rib-web components under isothermal closed-die forging. *Int J Adv Manuf Technol* 81(5):729–744
- Zhang DW, Yang H, Li HW, Fan XG (2012) Friction factor evaluation by FEM and experiment for TA15 titanium alloy in isothermal forming process. *Int J Adv Manuf Technol* 60(5–8):527–536
- Sun ZC, Yang H, Sun NG (2012) Effects of parameters on inhomogeneous deformation and damage in isothermal local loading forming of Ti-alloy component. *J Mater Eng Perform* 21(3):313–323
- Shen CW (2007) Research on material constitution models of TA15 and TC11 titanium alloys in hot deformation process. Master Thesis, Northwestern Polytechnical University
- Dutta A, Rao AV (1997) Simulation of isothermal forging of compressor disc by combined numerical and physical modeling techniques. *J Mater Process Technol* 72(3):392–395
- Zhang DW, Yang H, Sun ZC (2010) Analysis of local loading forming for titanium alloy T-shaped components using slab method. *J Mater Process Technol* 210(2):258–266

Publisher's note Springer Nature remains neutral with regard to jurisdictional claims in published maps and institutional affiliations.